THE JOURNAL OF PHYSICAL CHEMISTRY B

Article

pubs.acs.org/JPCB

Vesicle Structure and Formation of AB/BC Amphiphile Mixture Based on Hydrogen Bonding in a Selective Solvent: A Monte Carlo Study

Yuanyuan Han, Jie Cui, and Wei Jiang*

State Key Laboratory of Polymer Physics and Chemistry, Changchun Institute of Applied Chemistry, Chinese Academy of Sciences, Changchun 130022, P. R. China

Supporting Information

ABSTRACT: The effect of hydrogen bonding (H-bonding) on vesicle structure and its formation of the mixture of AB/BC amphiphilic molecules in a selective solvent for A and C blocks were studied using Monte Carlo simulation. For the purpose of comparison, H-bonding and covalent bonding were introduced via the two ends of two B blocks. The simulation results indicate that associative interaction of H-bonding (ε_{hb}) and repulsive interaction between A and C blocks (ε_{AC}) are the two key factors that determine vesicle structure. Four typical vesicles—symmetric, three-layer asymmetric, microphase-separated, and Janus vesicles—can be obtained through the adjustment of ε_{hb} and ε_{AC}. This result is interesting for experimental researchers for controlling vesicle structure and its properties through the introduction of H-bonding. More interestingly, the pathway of vesicle formation also depends on H-bonding. For an H-bonded system, the vesicle is more likely to be formed via diffusion of hydrophilic blocks into the center of spherical micelles. This process is independent of ε_{AC}. However, for a covalently bonded system, the vesicle is more likely to be formed via oblate membrane-closing for higher ε_{AC}. In addition, the vesicle is more likely to be formed via diffusion of hydrophilic blocks into the center of spherical micelles for lower ε_{AC}. Conformational investigation reveals that this H-bonding dependence results from the reversibility of H-bonding.

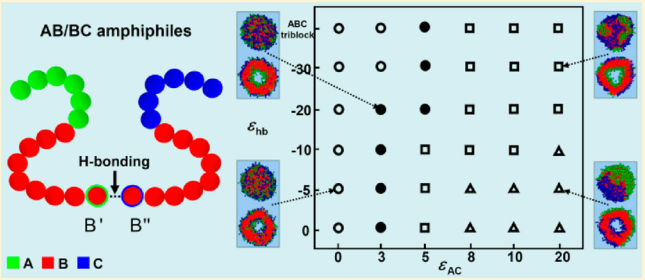

1. INTRODUCTION

Amphiphilic molecules can spontaneously self-assemble into micelles with various morphologies in selective solvents. Vesicles, which are included in these micelles, have attracted much attention.[1−6] A vesicle has spherical shell structure in which an aqueous compartment is enclosed by a bilayer membrane made of amphiphilic molecules. Because of this unique geometric structure, vesicles have been used to mimic natural cells and they are assumed to play an important role in biomedical sciences.[7−12] In general, natural cell membranes have a characteristic of bilayer asymmetry, that is, different chemical entities are located at the inner and outer layers. Therefore, an investigation on asymmetric vesicles is of both fundamental and practical importance.[11]

The ABC amphiphilic triblock copolymer, which consists of a middle hydrophobic block B and two hydrophilic blocks A and C, is a good candidate for the preparation of asymmetric vesicles.[13−16] However, the synthesis of a well-defined ABC triblock copolymer is generally complex and expensive. On the other hand, the self-assembly behavior of block copolymer mixture, in which different block copolymers can be held together by H-bonds, has many features in common with the covalently bonded copolymer system when the H-bonds are strong enough. Meanwhile, it is much easier to prepare H-bonding-based samples than to synthesize covalent analogues.[17] Therefore, interest in the self-assembly of block copolymer mixtures based on H-bonding[17−28] has been growing in the past few years. Matsushita et al.[18,19] investigated the phase behavior of AB/CD diblock copolymer mixture with complemental H-bonding chains in bulk. They found that the copolymer mixture self-assembled into some novel hierarchical structures which are difficult to determine from the simple block copolymer systems. Jiang et al.[20,21] reported the preparation of "pseudo-graft" copolymers based on H-bonding. Such pseudograft copolymers can form nanoaggregates in selective solvents. These nanoaggregates are highly sensitive to external stimuli because of H-bonding. Liu et al.[22,23] reported the preparation of "pseudo" ABC triblock copolymers from two diblock copolymers AB and BC with H-bonded B blocks. Many intriguing spherical micelles with Janus or flowerlike coronas were obtained. Recently, similar systems were studied by our group using Monte Carlo simulation.[25] The results revealed that the formation of corona patterns of spherical micelles depends on the competition between H-bonding interaction and repulsive interaction between the different hydrophilic blocks.

However, investigations regarding the preparation of the asymmetric vesicle based on H-bonding are still scarce thus far.

Received: January 31, 2012
Revised: June 30, 2012

   dx.doi.org/10.1021/jp3009783 | J. Phys. Chem. B XXXX, XXX, XXX−XXX

Schrage et al.[28] have found that typical asymmetric vesicles with different inner and outer amphiphilic surfaces can be formed by two diblock copolymers in a mixture based on electrostatic interaction, and they predicted that this type of vesicle can be obtained from copolymer mixtures based on H-bonding. Later, Kuo et al.[28] reported on asymmetric vesicles formed by a mixture of two diblock copolymers based on H-bonding, which confirmed the prediction of Schrage et al.

On the other hand, a detailed understanding of the kinetics of vesicle formation is important to the potential application of vesicles in biomedical sciences and can provide new insights into the origin of vesicles. In the past few years, the pathway of AB diblock or ABA triblock copolymer vesicle formation has been extensively investigated both experimentally and theoretically.[29−37] Among these investigations, computer simulation played an important role due to its advantages in tracking the self-assembly process and providing detailed information on the microstructure.[32−37] Previous simulation results indicate that the pathway of AB diblock or ABA triblock copolymer vesicle formation depends on many factors, such as the relative length of the hydrophilic blocks,[34] the interactions between the solvent and hydrophobic blocks,[36] the selective solvent addition rate,[37] and so on. However, to date, the effect of H-bonding on the kinetics of vesicle formation remains unclear. Thus, the current paper reports a lattice Monte Carlo simulation to investigate the effect of H-bonding on the structure and formation of asymmetric vesicles formed by AB/BC amphiphile mixture in a selective solvent for A and C blocks.

2. MODEL AND SIMULATION

The dynamic lattice Monte Carlo simulation method was used in this study. The system is embedded in a simple cubic lattice of volume $V = L \times L \times L$ with $L = 40$. Periodic boundary conditions are imposed in all three directions. The monomer concentration is 7%. Each monomer occupies one lattice site, and the monomers are self-avoiding and mutually avoiding, which insures that no more than one monomer existed per lattice site. The Larson type single-site bond fluctuation model[38−40] with the permitted bond length of 1 and $\sqrt{2}$ was used in these simulations, thus, each lattice site has 18 nearest neighbor sites in a three-dimensional space. The evolution of the chain configuration is achieved through the exchange move between monomer and solvent molecule. If the exchange move does not violate the bond length restriction and retains that no bond crossing occur, it is allowed. To enhance the efficiency, the partial-reptation algorithm, which has been proven suitable for studying the dynamic process,[33] is applied in the current paper. The microrelaxation modes are defined as follows: A monomer is randomly chosen to exchange with one of its 18 nearest neighbors. If the neighbor is a solvent molecule, exchange with the bead is attempted. If the exchange does not violate the bond length restriction, the exchange is allowed. This process constitutes a single movement. If the exchange would break two chain connections, it is not allowed. If the exchange creates a single break in the chain, the solvent molecule will continue to exchange with subsequent monomers along the chain until reconnection of the links occurs. The acceptance or rejection of the attempted move is further governed by the Metropolis importance sampling rule:[41] if the energy change ΔE is negative, the exchange is accepted. Otherwise, the exchange is accepted with a probability of $p = \exp[-\Delta E/(k_B T)]$, where $\Delta E = \sum_{ij} \Delta N_{ij} \varepsilon_{ij}$ is the energy change caused by the attempted move; ΔN_{ij} is the number difference of the nearest neighbor pairs between components i and j before and after the movement, where i, j = A, B, C, and solvent, respectively; ε_{ij} is the interaction energy between components i and j; k_B is the Boltzmann constant and assumed to be 1 in the whole simulation; and the parameter T is the reduced temperature.

The self-assembly of a mixture of coarse-grained chains, i.e., A_2-b-B_3/B_3-b-C_2, in a selective solvent for blocks A and C was considered in the current paper. The quantitative ratio of these two amphiphiles was fixed as 1:1. In order to mimic the "pseudo-triblock" copolymers based on H-bonding, there are functionalized monomers at the end of each hydrophobic chain, i.e., A_2-B_2-B′ and B″-B_2-C_2. Between these two types of functionalized monomers B′ and B″, there is associative interaction because of H-bonding. A detailed description of the model and algorithm for H-bonding can be found in a previous paper,[25] while a brief review is given as follows: A parameter q was introduced to reflect the number of possible internal orientational states within a functional monomer, and the probability of forming H-bonding between two nearest nonbonded functional monomers is $1/q$. Thus, the form of interaction energy between B′ and B″ in a Monte Carlo process is

$$\varepsilon_{B'B''} = \begin{cases} \varepsilon_{hb} & \text{if } \xi \le P_{hb} \\ \varepsilon_{BB} & \text{otherwise} \end{cases} \quad (1)$$

where ξ is a random number between 0 and 1; ε_{hb} and ε_{BB} are the associative interaction of H-bonding and the ordinary van der Waals interaction between B blocks, respectively; P_{hb} is the probability of forming H-bonding between two nearest nonbonded functional monomers. Due to the extremely directional dependency of H-bonding, P_{hb} would be very small. According to the work of Huh et al.,[42,43] P_{hb} was set to be 10% (i.e., $q = 10$) in the current study. Once the H-bonding is formed, it will be maintained unless the movement of the bonded functional monomer violates the bond length restriction of H-bonding. This condition means that the probability of breaking H-bonding mainly depends on the associative interaction of H-bonding. When the associative interaction is strong, the possibility of breaking H-bonding is relatively low due to the strong energy constraint for the functional monomers.

In the current study, the interaction parameters were set to be $\varepsilon_{AS} = \varepsilon_{CS} = -1$, which means that blocks A and C are hydrophilic and their hydrophilicities are the same. According to the experimental[44] and simulation results,[45] the amphiphilic block copolymers with strong hydrophobicities tend to form vesicles in selective solvent. Therefore, ε_{BS} was set to be 6 corresponding to the strong hydrophobicity of block B. ε_{AB} and ε_{BC} were set to be 1 to mimic the incompatibilities between different blocks. ε_{AC} was set as positive corresponding to the repulsive interaction between blocks A and C. ε_{hb} was set as negative corresponding to the H-bonding interaction between B′ and B″. All other self-interaction parameters between the same components (i.e., ε_{AA}, ε_{BB}, ε_{CC}, and ε_{SS}) were set to be 0. The annealing method was implemented. The inverse temperature $1/T$ was set to be 0 at first to mimic the homogeneous state. Then it was changed gradually from 0 to 0.07 representing that the system was annealing to a relatively low temperature. The annealing rate (i.e., the increasing rate of $1/T$) was set to be 0.0002 per 9000 Monte Carlo steps (MCS). The purpose for choosing 9000 MCS is to make sure that the

dx.doi.org/10.1021/jp3009783 | J. Phys. Chem. B XXXX, XXX, XXX−XXX

system is fully relaxed at each temperature during the annealing. In one MCS, on the average, each monomer has attempted one exchange move. After 3.15×10^6 MCS, keeping $1/T = 0.07$ unchanged, another 3.15×10^6 MCS were carried out to confirm that the final structures are in an equilibrium state.

3. RESULTS AND DISCUSSION

The current study mainly focuses on vesicles formed by A_2B_3/B_3C_2 amphiphile mixtures based on H-bonding. The associative interaction of H-bonding ε_{hb} and the repulsive interaction between A and C blocks ε_{AC} are variable. The simulation results are given in two parts: section 3.1 describes the effects of ε_{hb} and ε_{AC} on the vesicle membrane structures, and section 3.2 examines the formation mechanisms of the vesicles obtained in section 3.1. The effects of ε_{hb} and ε_{AC} on the pathway of vesicle formation are revealed. Noteworthy, the interpretation of the dynamic process of vesicle formation is valid only for the sequence of Monte Carlo moves used in the current paper. In all snapshots and schematic diagrams, blocks A, B, and C are represented by blue, red, and green, respectively.

3.1. Effect of H-Bonding on Vesicle Structure. An ultimate condition of H-bonding, that is, $\varepsilon_{hb} = -\infty$, is first investigated. In this condition, A_2B_3 and B_3C_2 amphiphiles are actually covalently bonded, forming $A_2B_6C_2$ amphiphiles. The simulation results are given in Figure 1. The insoluble block B

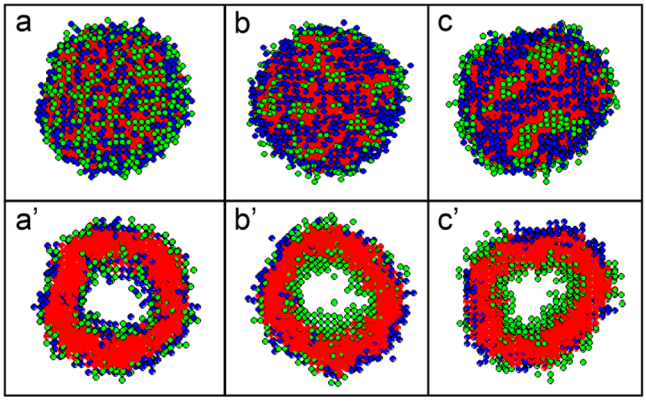

Figure 1. Membrane structures of the vesicles formed by $A_2B_6C_2$ amphiphiles as a function of ε_{AC}: (a) $\varepsilon_{AC} = 0$, (b) $\varepsilon_{AC} = 5$, (c) $\varepsilon_{AC} = 10$; a′−c′ are the cross sections corresponding to a−c, respectively.

forms the hydrophobic midlayer of the vesicle, whereas the soluble blocks A and C form the hydrophilic surface. Patterns on the hydrophilic surfaces obviously changed with the increase in ε_{AC}. When ε_{AC} is zero, a uniform mixing of blocks A and C in both the inner and outer hydrophilic surfaces, that is, a symmetric vesicle, is observed in Figures 1a and 1a′. However, when ε_{AC} is increased to 5, blocks A and C become phase separated. Figures 1b and 1b′ show that the inner surface of the vesicle is occupied almost completely by block C, while the outer surface is still occupied by the mixture of blocks A and C. Block A is the major component in the outer surface. Therefore, an ABC three-layer asymmetric vesicle is formed. When ε_{AC} is further increased to 10, the outer surface exhibits a microphase-separated structure attributed to the strong repulsion between blocks A and C (Figure 1c).

For the purpose of comparison, the other ultimate condition of H-bonding, that is, $\varepsilon_{hb} = 0$, is also simulated. Figure 2a shows that the symmetric vesicle is obtained for $\varepsilon_{AC} = 0$, which is similar to that in Figure 1a. However, when $\varepsilon_{AC} = 5$, the phase

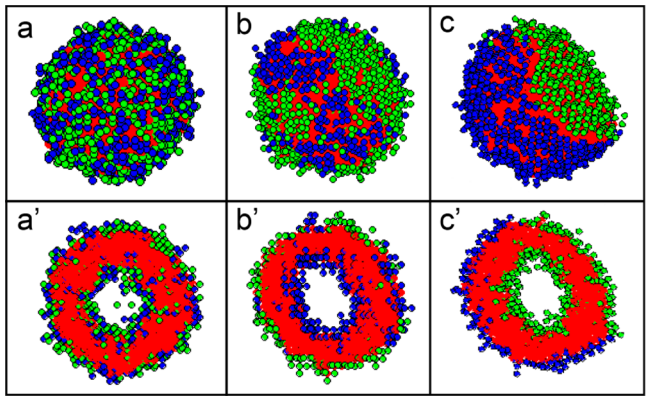

Figure 2. Membrane structures of the vesicles formed by A_2B_3/B_3C_2 amphiphile mixture based on H-bonding for $\varepsilon_{hb} = 0$ as a function of ε_{AC}: (a) $\varepsilon_{AC} = 0$, (b) $\varepsilon_{AC} = 5$, (c) $\varepsilon_{AC} = 10$; a′−c′ are the cross sections corresponding to a−c, respectively. It is equally likely that block A or C forms the inner layer.

separation between blocks A and C is much stronger than that in the covalently bonded system, that is, the microphase-separated structure in the outer surface (Figure 2b) is formed instead of the uniform mixing of blocks A and C (Figure 1b). When ε_{AC} is further increased to 10, the vesicle structure becomes totally different. Figure 2c shows that the outer surface exhibits a Janus-type pattern attributed to the macrophase separation between blocks A and C. In addition, the inner surface is occupied by block C when $\varepsilon_{AC} = 10$ (Figure 2c′), and it is occupied by block A when $\varepsilon_{AC} = 5$ (Figure 2b′). This phenomenon results from the same characteristic of blocks A and C. More than 10 initial states are randomly selected. The possibility for either block A or C occupying the inner surface is found to be equal.

Based on the above simulation results, the vesicle structure depends on the bonding type and the repulsive interaction between blocks A and C (ε_{AC}). To further probe the effects of ε_{hb} and ε_{AC} on the vesicle membrane structure, a morphological diagram for a wide range of interaction parameters ε_{hb} and ε_{AC} is given in Figure 3. Typical vesicle morphologies and their cross sections are given in Figures 3a to 3d. This diagram shows

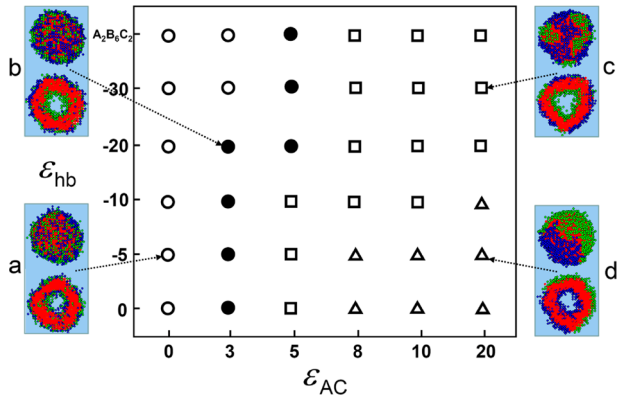

Figure 3. Diagram of the vesicle structures formed by A_2B_3/B_3C_2 amphiphile mixture based on H-bonding as functions of ε_{hb} and ε_{AC}. The same symbols represent the similar vesicle structures. Representative snapshots of the vesicles and their cross sections are shown in a−d: (a) symmetric vesicle, (b) three-layer asymmetric vesicle, (c) microphase separated asymmetric vesicle, (d) Janus-type asymmetric vesicle.

dx.doi.org/10.1021/jp3009783 | J. Phys. Chem. B XXXX, XXX, XXX−XXX

that the symmetric vesicles are observed when $\varepsilon_{AC} < 3$, whereas the asymmetric vesicles are observed when $\varepsilon_{AC} > 3$. Moreover, the regions of asymmetric vesicles with varied membrane structures are also observed in this diagram. The three-layer asymmetric vesicles (Figure 3b) can be formed for lower ε_{AC} values, whereas asymmetric vesicles with either microphase-separated outer surface (Figure 3c) or Janus-type outer surface (Figure 3d) can be formed for higher ε_{AC} values. On the other hand, the outer surface of the vesicle tends to change from the microphase-separated (Figure 3c) to the Janus-type (Figure 3d) structure with decreasing interaction of H-bonding for higher ε_{AC} values. This diagram reflects that ε_{AC} is crucial to the formation of asymmetric vesicle. Phase separation between blocks A and C can occur to form asymmetric vesicle when ε_{AC} is strong enough. On the other hand, ε_{hb} is the key factor in determining the pattern of the outer surface. Microphase separation will occur to form a microphase-separated outer surface when ε_{hb} is strong. Meanwhile, macrophase separation will occur to form a Janus-type outer surface when ε_{hb} is weak. Note that the three-layer asymmetric vesicle has been observed both in experiment[16] and in simulation,[13] whereas the Janus and microphase-separated asymmetric vesicles are seldom to be observed thus far. This study may provide a new clue for preparing structure-controlled asymmetric vesicles via the adjustment of H-bonding interaction.

The fraction of H-bonded amphiphiles (ϕ_{hb}) is introduced to elucidate the effect of ε_{hb} and ε_{AC} on the vesicle membrane structure. All values for ϕ_{hb} are counted after the vesicle structure becomes stable. Figure 4 shows the variations of ϕ_{hb}

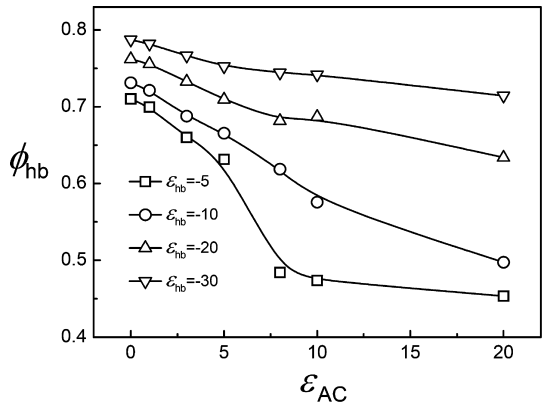

Figure 4. Variations of ϕ_{hb} with ε_{AC} for the A_2B_3/B_3C_2 amphiphile mixture based on H-bonding.

with ε_{AC} for different ε_{hb}. ϕ_{hb} rapidly decreases with an increase in ε_{AC} when the interaction of H-bonding is weak ($\varepsilon_{hb} \geq -10$). An increase in ε_{AC} can break the H-bonding association between the two amphiphiles in the case of weak H-bonding interaction. This results in a macrophase separation between blocks A and C. However, ϕ_{hb} maintains a relatively high value with an increase in ε_{AC} when the interaction of H-bonding is strong ($\varepsilon_{hb} \leq -20$). Most of the amphiphiles are connected by H-bonding, which restrains the macrophase separation between blocks A and C. Thus, only microphase separation is observed for strong H-bonded systems.

3.2. Pathway of Spontaneous Vesicle Formation. The vesicle formation of $A_2B_6C_2$ amphiphiles is investigated first. Figure 5 shows the evolution of $A_2B_6C_2$ amphiphiles when $\varepsilon_{AC} = 0$ and $\varepsilon_{AC} = 20$. Figure 5a shows that, when $\varepsilon_{AC} = 0$, the amphiphiles first aggregate into a large irregular sphere (Figure $5a_1$), in which the hydrophilic blocks A and C are randomly distributed (Figure $5a_2$). Then, some hydrophilic blocks in the big irregular sphere diffuse toward the surface, while some hydrophilic blocks diffuse toward the center (Figures $5a_3$ to $5a_4$), forming a symmetric vesicle (Figure $5a_5$). However, when $\varepsilon_{AC} = 20$, the pathway of vesicle formation is totally different, as shown in Figure 5b. The amphiphiles first form a big oblate membrane (Figure $5b_1$); then, the oblate membrane tends to bend (cross sections of the bended membranes are shown in Figures $5b_2$ to $5b_3$). Finally, the membrane closes up to form an asymmetric vesicle (Figures $5b_4$ to $5b_5$). A series of ε_{AC} values between 0 and 20 are employed to systematically study the effect of ε_{AC}. The detailed simulation results are given in Figure S1 in the Supporting Information. Vesicle is formed via the diffusion of hydrophilic blocks in a big irregular sphere when $\varepsilon_{AC} \leq 8$. Meanwhile, vesicle is formed via oblate membrane closing when $\varepsilon_{AC} \geq 9$.

To understand the above phenomenon in microscale, the average end-to-end distance of block B ($\bar{R}_B$) is introduced. Note that 10 initial states are randomly selected, $\bar{R}_B$ in each system with different initial states is calculated, and the values of $\bar{R}_B$ reported in the current paper are the mean values of these 10 systems. Figure 6 shows the variations in $\bar{R}_B$ with simulation time (t) for different values of ε_{AC}. When $\varepsilon_{AC} = 0$, $\bar{R}_B$ rapidly drops with increasing time as high as $t = 9.0 \times 10^5$ MCS and remains almost unchanged with further increase in time. However, $\bar{R}_B$ first decreases and then increases considerably to a high value, and finally remains almost unchanged with increasing time for $\varepsilon_{AC} = 5$ and $\varepsilon_{AC} = 20$. An increase in $\bar{R}_B$ means that the chains tend to be more stretched. Moreover, the increase speed of $\bar{R}_B$ for $\varepsilon_{AC} = 20$ is much faster than that for $\varepsilon_{AC} = 5$. To further understand the effect of ε_{AC} on the vesicle formation of $A_2B_6C_2$ amphiphiles, the average distance from each B monomer to the mass center of all amphiphiles ($\bar{D}_B$) is introduced, and the values of $\bar{D}_B$ reported in the current paper are also the mean values of 10 systems with different initial states. $\bar{D}_B$ can reflect the aggregation degree of the amphiphiles. Figure 7 shows the variations in $\bar{D}_B$ with simulation time (t) for different ε_{AC}. $\bar{D}_B$ decreases considerably with increasing time for all ε_{AC}, indicating that the chains form a dense aggregation. The decrease speed of $\bar{D}_B$ becomes much slower with increasing ε_{AC}. Thus, an increase in ε_{AC} can slow down the aggregating speed of the amphiphiles. An increase in ε_{AC} leads to an increase in the chain-stretching speed on the one hand and results in the decrease in the chain-aggregating speed on the other hand. That is to say, the chains tend to stretch rapidly while aggregating slowly for strong ε_{AC}, and tend to stretch slowly while aggregating rapidly for weak ε_{AC}. Therefore, when ε_{AC} is strong, the chains are stretched before the aggregation is formed. These stretched chains tend to array parallel to each other to minimize energy, forming big oblate membranes at the early stage of the evolution. This can be confirmed by the typical micelle morphologies shown in Figures 6 and 7. Figure 7b shows that the big oblate membrane is formed when $t = 1.29 \times 10^6$ MCS, with the chains highly stretched at this time (Figure 6b). However, the aggregating speed of the chains is so fast that the big irregular sphere is quickly formed at $t = 1.08 \times 10^6$ MCS when $\varepsilon_{AC} < 9$ (Figure 7a) before the chains become stretched (Figure 6a). Therefore, the pathway for vesicle formation is a result of a competition between chain-aggregating and chain-stretching.

For the H-bonded A_2B_3/B_3C_2 amphiphile mixture systems, Figure 8 shows the pathway of spontaneous vesicle formation

dx.doi.org/10.1021/jp3009783 | J. Phys. Chem. B XXXX, XXX, XXX−XXX

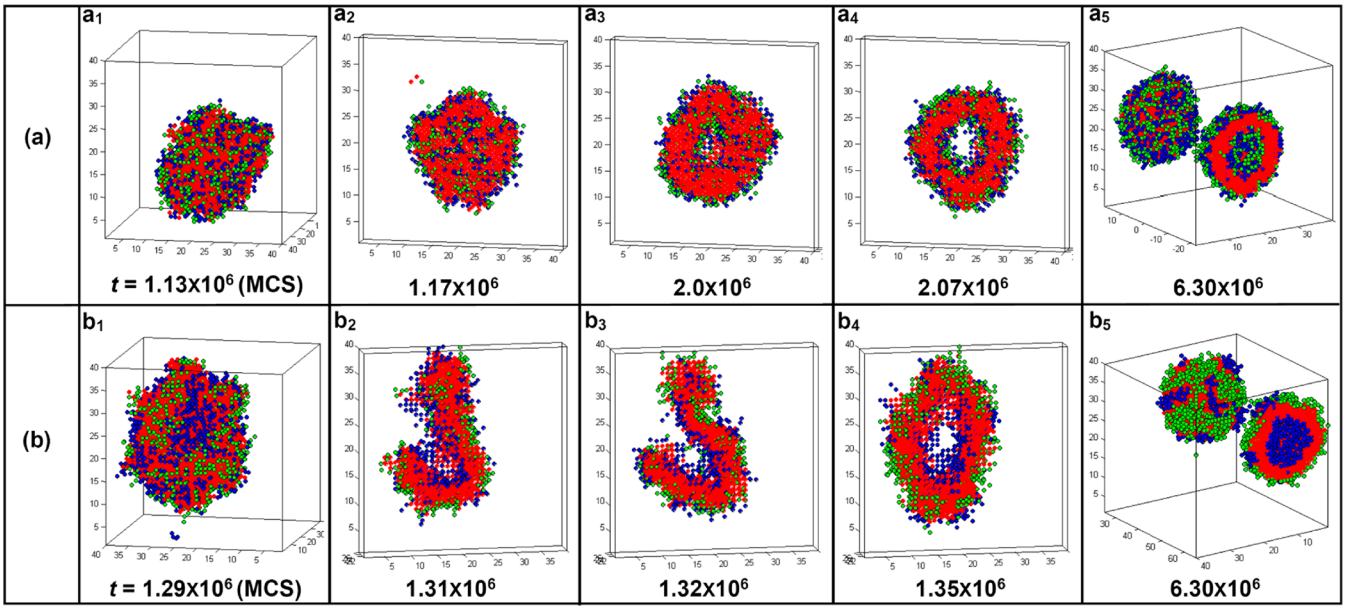

Figure 5. Snapshots showing the pathways of spontaneous vesicle formation of $A_2B_6C_2$ amphiphiles: (a) $\varepsilon_{AC} = 0$, (b) $\varepsilon_{AC} = 20$. The simulation time is labeled below each snapshot. For the purpose of clarity, the cross sections of the micelles are given in a_2–a_4 and b_2–b_4.

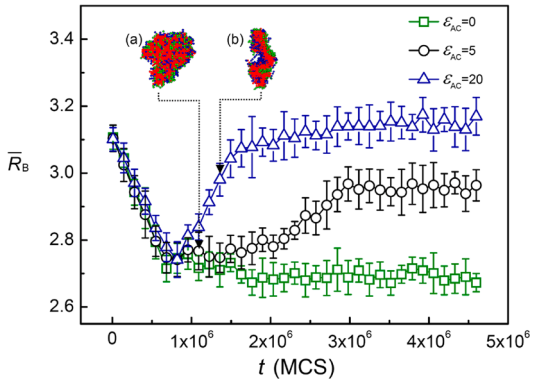

Figure 6. Variations of $\overline{R}_B$ with simulation time for $A_2B_6C_2$ amphiphiles at different values of ε_{AC}. Cross sections of the typical micelles are given in a and b: (a) $\varepsilon_{AC} = 5$, $t = 1.08 \times 10^6$ MCS; (b) $\varepsilon_{AC} = 20$, $t = 1.29 \times 10^6$ MCS.

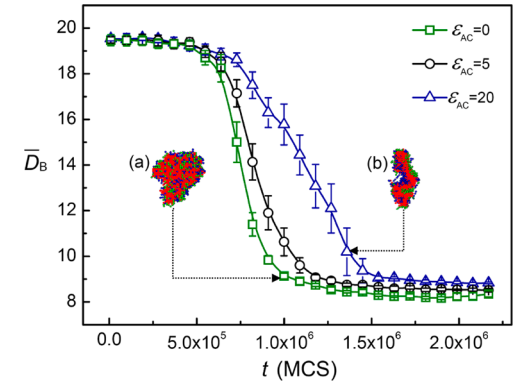

Figure 7. Variations of $\overline{D}_B$ with simulation time for $A_2B_6C_2$ amphiphiles at different values of ε_{AC}. Cross sections of the typical micelles are given in a and b: (a) $\varepsilon_{AC} = 5$, $t = 1.08 \times 10^6$ MCS; (b) $\varepsilon_{AC} = 20$, $t = 1.29 \times 10^6$ MCS.

for $\varepsilon_{hb} = -30$, $\varepsilon_{AC} = 20$. The vesicle is formed via the diffusion of hydrophilic blocks in the big irregular sphere. This is totally different from that of $A_2B_6C_2$ amphiphiles observed when $\varepsilon_{AC} = 20$ (Figure 5b). Moreover, vesicle formations for various values of ε_{hb} and ε_{AC} (i.e., $\varepsilon_{AC} = 0$ to 20 and $\varepsilon_{hb} = 0$ to -30) are investigated in the H-bonded systems. The simulation results show that the vesicle is formed via the diffusion of hydrophilic blocks in the big irregular sphere (Figures S2 to S4 in the Supporting Information), which is in common with that when ε_{AC} is weak for $A_2B_6C_2$ amphiphiles (Figure 5a). In other words, the pathway of vesicle formation for the A_2B_3/B_3C_2 amphiphile mixture based on H-bonding is independent of ε_{AC}. $\overline{R}_B$ for the A_2B_3/B_3C_2 amphiphile mixture is calculated to illustrate this phenomenon. Figure 9 shows the variations in $\overline{R}_B$ with simulation time at $\varepsilon_{hb} = -30$ for $\varepsilon_{AC} = 0$ and $\varepsilon_{AC} = 20$. The two curves for different ε_{AC} overlap each other, indicating that $\overline{R}_B$ does not depend on ε_{AC} during vesicle formation. This is different from the simulation results observed for $A_2B_6C_2$ amphiphiles shown in Figure 6. This difference can be attributed to the reversibility of H-bonding. A schematic diagram showing the possible chain conformation for the two systems is given in Figure 10. At the early stage, the chains tend to shrink in both systems (Figures 10a and 10c) caused by the hydrophobic interactions between block B and the solvents. As time increases, the chains tend to be stretched because of the strong repulsion between blocks A and C in covalently bonded systems (Figure 10b). However, in the system where the two amphiphiles are connected via H-bonding (Figure 10d), the strong repulsion between blocks A and C can break H-bonding. Thus, the chains cannot be stretched further because of the reversibility of H-bonding, as shown in Figure 10e. As a result, only one pathway of the vesicle formation for the H-bonded system is observed.

4. CONCLUSION

Monte Carlo simulation was used to study the effect of H-bonding on vesicle structure and its formation of A_2B_3/B_3C_2 amphiphile mixture based on H-bonding in a selective solvent for blocks A and C. For the purpose of comparison, the covalently bonded system (i.e., $A_2B_6C_2$ amphiphiles) was also

dx.doi.org/10.1021/jp3009783 | J. Phys. Chem. B XXXX, XXX, XXX–XXX

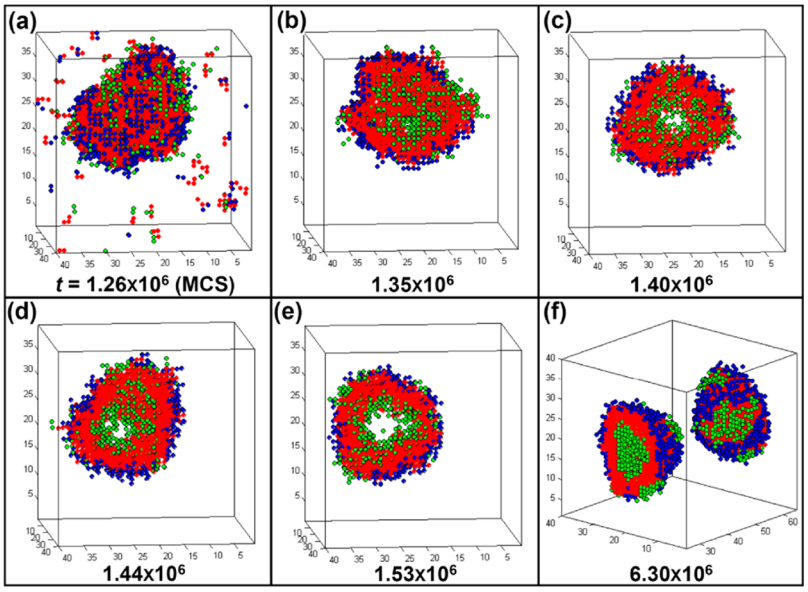

Figure 8. Snapshots showing the pathway of spontaneous vesicle formation of A_2B_3/B_3C_2 amphiphile mixture based on H-bonding for $\varepsilon_{hb} = -30$ and $\varepsilon_{AC} = 20$. The simulation time is labeled below each snapshot. For the purpose of clarity, the cross sections of the micelles are given in b–e.

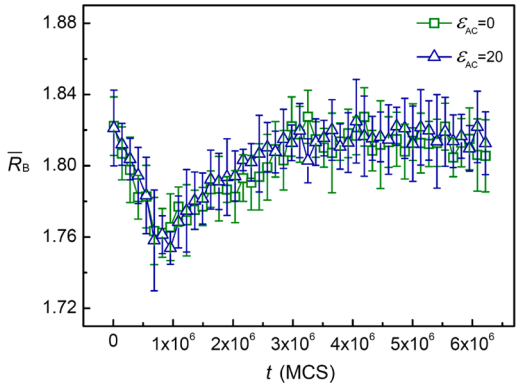

Figure 9. Variations of $\overline{R}_B$ with simulation time for A_2B_3/B_3C_2 amphiphile mixture based on H-bonding at different values of ε_{AC} for $\varepsilon_{hb} = -30$.

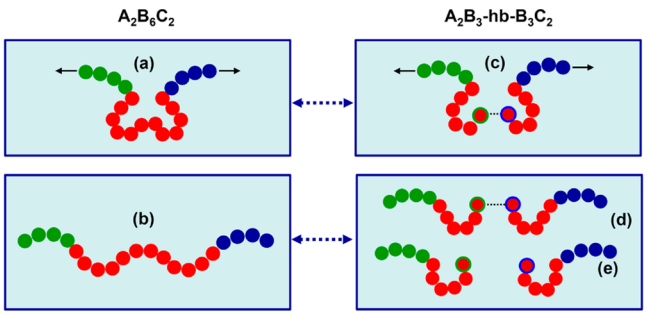

Figure 10. Illustration of the chain conformations: (a, b) $A_2B_6C_2$ amphiphiles; (c–e) A_2B_3/B_3C_2 amphiphile mixture based on H-bonding.

investigated in the current paper. ε_{hb} and ε_{AC} are the two key factors that determine vesicle structure. Four typical vesicles, namely, symmetric, three-layer asymmetric, microphase-separated, and Janus-type asymmetric vesicles, can be obtained through the adjustment of ε_{hb} and ε_{AC}. More interestingly, the pathway of vesicle formation also depends on H-bonding. For the H-bonded system, the vesicle is more likely to be formed via the diffusion of the hydrophilic blocks into the center of spherical micelles, and this process is independent of ε_{AC}. However, for the covalently bonded system, the vesicle is more likely to be formed via oblate membrane closing for higher ε_{AC} values. Meanwhile, the vesicle is more likely to be formed via the diffusion of the hydrophilic blocks into the center of spherical micelles for lower ε_{AC} values. The conformation study reveals that the chain-stretching speed and chain-aggregating speed for the $A_2B_6C_2$ amphiphiles depend on ε_{AC}, and the pathway for the vesicle formation is a result of the competition between these two speeds. However, for the H-bonded system, chain conformation is independent of ε_{AC} because of the reversibility of H-bonding, that is, no competing effect between chain stretching and chain-aggregating exists in this system. This leads to only one pathway observed.

■ ASSOCIATED CONTENT

Ⓢ Supporting Information

Simulative results of the vesicle formation process of $A_2B_6C_2$ amphiphiles and A_2B_3/B_3C_2 amphiphile mixture based on H-bonding. This material is available free of charge via the Internet at http://pubs.acs.org.

■ AUTHOR INFORMATION

Corresponding Author

*E-mail: wjiang@ciac.jl.cn. Tel: +86-431-85262151. Fax: +86-431-85262126.

Notes

The authors declare no competing financial interest.

■ ACKNOWLEDGMENTS

Financial support was provided by the National Natural Science Foundation of China for Youth Science Funds (21004063), Major Program (50930001), Outstanding Young Investigators (50725312), Creative Research Groups (50921062), and the National Basic Research Program (2007CB808000) of China.

■ REFERENCES

(1) Ding, J.; Liu, G. *Macromolecules* **1997**, *30*, 655–657.

(2) Discher, D. E.; Eisenberg, A. *Science* **2002**, *297*, 967−973.
(3) Soo, P. L.; Eisenberg, A. *J. Polym. Sci., Part B: Polym. Phys.* **2004**, *42*, 923−938.
(4) Zhu, J.; Jiang, Y.; Liang, H.; Jiang, W. *J. Phys. Chem. B* **2005**, *109*, 8619−8625.
(5) Kong, W.; Li, B.; Jin, Q.; Ding, D. *Langmuir* **2010**, *26*, 4226−4232.
(6) Wang, H.; Liu, Y.-T.; Qian, H.-J.; Lu, Z.-Y. *Polymer* **2011**, *52*, 2094−2101.
(7) Kita-Tokarczyk, K.; Grumelard, J.; Haefele, T.; Meier, W. *Polymer* **2005**, *46*, 3540−3563.
(8) Zhou, Y.; Yan, D. *J. Am. Chem. Soc.* **2005**, *127*, 10468−10469.
(9) Zhou, Y.; Yan, D. *Angew. Chem., Int. Ed.* **2005**, *44*, 3223−3226.
(10) Li, X.; Liu, Y.; Wang, L.; Deng, M.; Liang, H. *Phys. Chem. Chem. Phys.* **2009**, *11*, 4051−4059.
(11) Blanazs, A.; Armes, S. P.; Ryan, A. J. *Macromol. Rapid Commun.* **2009**, *30*, 267−277.
(12) Malinova, V.; Belegrinou, S.; de Bruyn Ouboter, D.; Meier, W. *Adv. Polym. Sci.* **2010**, *224*, 113−165.
(13) Cui, J.; Jiang, W. *Langmuir* **2010**, *26*, 13672−13676.
(14) Stoenescua, R.; Meier, W. *Chem. Commun.* **2002**, 3016−3017.
(15) Liu, F.; Eisenberg, A. *J. Am. Chem. Soc.* **2003**, *125*, 15059−15064.
(16) Njikang, G.; Han, D.; Wang, J.; Liu, G. *Macromolecules* **2008**, *41*, 9727−9735.
(17) ten Brinke, G.; Ruokolainen, J.; Ikkala, O. *Adv. Polym. Sci.* **2007**, *207*, 113−177.
(18) Asari, T.; Matsuo, S.; Takano, A.; Matsushita, Y. *Macromolecules* **2005**, *38*, 8811−8815.
(19) Dobrosielska, K.; Takano, A.; Matsushita, Y. *Macromolecules* **2010**, *43*, 1101−1107.
(20) Chen, D.; Jiang, M. *Acc. Chem. Res.* **2005**, *38*, 494−502.
(21) Guo, M.; Jiang, M. *Soft Matter* **2009**, *5*, 495−500.
(22) Hu, J.; Liu, G. *Macromolecules* **2005**, *38*, 8058−8065.
(23) Yan, X.; Liu, G.; Hu, J.; Willson, C. G. *Macromolecules* **2006**, *39*, 1906−1912.
(24) Gao, W.-P.; Bai, Y.; Chen, E-Q.; Li, Z.-C.; Han, B.-Y.; Yang, W.-T.; Zhou, Q.-F. *Macromolecules* **2006**, *39*, 4894−4898.
(25) Han, Y.; Jiang, W. *J. Phys. Chem. B* **2011**, *115*, 2167−2172.
(26) Lefevre, N.; Fustin, C.-A.; Gohy, J.-F. *Macromol. Rapid Commun.* **2009**, *30*, 1871−1888.
(27) Schrage, S.; Sigel, R.; Schlaad, H. *Macromolecules* **2003**, *36*, 1417−1420.
(28) Kuo, S.-W.; Tung, P.-H.; Chang, F.-C. *Eur. Polym. J.* **2009**, *45*, 1924−1935.
(29) Yu, K.; Eisenberg, A. *Macromolecules* **1998**, *31*, 3509−3518.
(30) Chen, L.; Shen, H.; Eisenberg, A. *J. Phys. Chem. B* **1999**, *103*, 9488−9497.
(31) Battaglia, G.; Ryan, A. J. *J. Phys. Chem. B* **2006**, *110*, 10272−10279.
(32) Yamamoto, S.; Maruyama, Y.; Hyodo, S.-a. *J. Chem. Phys.* **2002**, *116*, 5842−5849.
(33) Ji, S.; Ding, J. *Langmuir* **2006**, *22*, 553−559.
(34) He, X.; Schmid, F. *Macromolecules* **2006**, *39*, 2654−2662.
(35) He, X.; Schmid, F. *Phys. Rev. Lett.* **2008**, *100*, 137802.
(36) Huang, J.; Wang, Y.; Qian, C. *J. Chem. Phys.* **2009**, *131*, 234902.
(37) Han, Y.; Yu, H.; Du, H.; Jiang, W. *J. Am. Chem. Soc.* **2010**, *132*, 1144−1150.
(38) Carmesin, I.; Kremer, K. *Macromolecules* **1988**, *21*, 2819−2823.
(39) Larson, R. G.; Scriven, L. E.; Davis, H. T. *J. Chem. Phys.* **1985**, *83*, 2411−2420.
(40) Larson, R. G. *J. Chem. Phys.* **1989**, *91*, 2479−2488.
(41) Metropolis, N.; Rosenbluth, A. W.; Rosenbluth, M. N.; Teller, A. H.; Teller, E. *J. Chem. Phys.* **1953**, *21*, 1087−1092.
(42) Huh, J.; Ikkala, O.; ten Brinke, G. *Macromolecules* **1997**, *30*, 1828−1835.
(43) Huh, J.; ten Brinke, G. *J. Chem. Phys.* **1998**, *109*, 789−797.
(44) Shen, H.; Eisenberg, A. *J. Phys. Chem. B* **1999**, *103*, 9473−9487.
(45) Sun, P.; Yin, Y.; Li, B.; Chen, T.; Jin, Q.; Ding, D.; Shi, A.-C. *J. Chem. Phys.* **2005**, *122*, 204905.